

Strong to weak localization transition and two-parameter scaling in a two-dimensional quantum dot array

N. P. Stepina,* E. S. Koptev, A. V. Dvurechenskii, and A. I. Nikiforov
Institute of Semiconductor Physics, 630090 Novosibirsk, Russia

(Received 5 March 2009; revised manuscript received 3 August 2009; published 11 September 2009)

The transition from strong to weak localization behavior was observed in two-dimensional Ge/Si quantum dot structure under the variation in the quantum dot occupancy, their areal density and annealing of the structures at 480–625 °C. To clarify the carrier transport mechanism and separate the hopping and diffusive regimes, the temperature dependence of conductance and conductance nonlinearity were analyzed in the structures with different correlations between the disorder and interaction. It was shown that the change in the relative disorder without significantly changing the interaction keeps the system inside the one-parameter scaling. The role of the interaction in two-parameter scaling was revealed by observing the shift of Gell-Mann-Low scaling function for the samples with large variation in the Coulomb interaction.

DOI: [10.1103/PhysRevB.80.125308](https://doi.org/10.1103/PhysRevB.80.125308)

PACS number(s): 73.20.Fz, 73.61.Ey, 73.21.La

I. INTRODUCTION

According to the Anderson model,¹ the transition from localized to delocalized state in a three-dimensional disordered system is driven by the relative disorder $Z=I/W$, where W is the energy levels dispersion and $I=\int\psi_1^*\hat{H}\psi_2d^3r$ is the hopping integral. The transition occurs when the parameter Z increases over some critical value $(I/W)_{crit}$. In the opposite case of $Z<(I/W)_{crit}$ the electron wave functions at the Fermi level remain localized, making the system an Anderson insulator.

To describe the transport behavior of disordered systems, the authors² proposed a one-parameter scaling theory in which the disorder parameter determining the system state was found to coincide with the nondimensional (in units of e^2/h) conductance G . The case of two dimensions (2D) was shown to be a special in that it is the lower critical dimensionality for the metal-insulator transition (MIT) in disordered systems: in three-dimensional case, both metallic and insulating states may exist, whereas in one dimensional case any small disorder causes localization.

To clarify the possibility of MIT transition in 2D, over two decades there was a high theoretical activity based on expansions around 2D. Scaling theory of localization prohibits the existence of extended electronic states in 2D at absolute zero in the presence of disorder. Arguments based on the scaling theory indicate that as $T\rightarrow 0$, resistivity always increases, exponentially in the case of strong localization (SL) or logarithmically in the case of weak localization (WL).² The sheet resistance determines whether the system falls into the SL or WL regime. Following the experiments^{3–5} performed on a high-mobility 2D electron-gas system (2DES) in zero magnetic field several groups have presented fairly convincing evidence for the existence of a true MIT in 2D.

The conflict with the scaling theory of localization has been partially resolved by Finkelstein⁶ and Punnose and Finkelstein,⁷ who showed theoretically that two, instead of one-parameter scaling defines the system state, with one scaling variable being governed by disorder, and the other, by the electron-electron (e-e) interaction. In spite of the extensive theoretical work, done to prove that the e-e interac-

tion can indeed induce delocalization in 2D disordered systems,^{8–10} no conclusive experimental evidence for this phenomenon has been reported so far. For such evidence to be gained, the e-e interaction and the disorder have to be varied independently. However, in the majority of reported studies, MIT was observed while varying just one parameter, the carrier concentration N_c , affecting both the disorder and the interaction. In spite of this, D. A. Knyazev *et al.*¹¹ and S. Anissimova *et al.*¹² could manage to describe the transport properties of 2DES with two scaling parameters when varying the carrier concentration and the measurement temperature only with¹² and without¹¹ magnetic field; they, however, failed to reveal the independent contributions to transport regime due to the e-e interaction and disorder.

In the present study, the scaling hypothesis was scrutinized when studying the conductance behavior in 2D tunnel-coupled Ge quantum dots in Si at different correlations between the disorder and e-e interaction. In contrast to the majority of 2DES studies, we varied several experimental parameters that had different influence on the disorder and the e-e interaction. A characteristic feature of the Ge/Si quantum dots (QDs) system is that, unlike in 2DES, where the carrier localization is caused by impurity-induced fluctuating potential, the localization of holes in QD plane results from the structural disorder originating from the size dispersion of QDs and their random distribution in the growth plane. This kind of disorder is expected to be independent of the carrier concentration, QD composition, and array density. So, high-resolution transmission electron microscopy and scanning tunnel microscope images for the samples with different QD density (4×10^{11} cm⁻² and 8×10^{11} cm⁻²) have practically the same size dispersion ($\sim 15\%$). Doping of the QD array changes the value of Z via the hopping integral and modifies the Coulomb interaction between QDs. Both the hopping integral and the e-e interaction vary nonmonotonically with the doping level due to nonmonotonic dependence of the density of states on energy. In this situation, the Coulomb interaction attains its highest value when the ground and excited states of QDs become fully filled with charge carriers, whereas the hopping integral vanishes owing to the corresponding decrease in the density of states.

Changing the QD array density, their size and composition simultaneously with the variation in the dot filling factor, one can obtain QD structures with a broad range of correlations between the relative disorder Z and the interaction. This in turn makes it possible to test the scaling hypothesis and identify parameters that determine the transport regime of the system. Variation in several parameters drives the system not along the single trajectory, as in,^{11,12} but via some area of the plane of two scaling parameters. To carefully check the scaling hypothesis, one has to provide for a sufficiently wide range of conductance values in the system. It has been shown recently^{13,14} that hopping conductance, which determines the charge-transport mechanism in Ge/Si QD arrays at low temperatures (≤ 20 K), broadly varies, from 4×10^{-6} to 6×10^{-12} Ohm⁻¹, when the filling factor of QDs with holes ν increases from 0.5 to 6. Moreover, not only the conductance, but also the localization radius ξ in this system was shown¹⁵ to be substantially dependent on ν , with ξ —values varying by more than one order of magnitude as we pass from full- to half-filled QD ground state. Normally, the localization radius increases strongly in the vicinity of the transition point, suggesting that the transport regimes of the Ge/Si QDs system will undergo changes at further increase in ξ .

Three ways to vary the disorder, the hopping integral, and the interaction force, all inducing changes in the conductance and in the ξ value, were proposed and realized in this work. First, the average number of holes in QD was varied by the boron concentration in the δ -doped Si layer inserted 5 nm below the QD layer. Second, to enhance the hopping integral I and the interaction without significant change in W , the QD array density value was increased from 4×10^{11} cm⁻² to 8×10^{11} cm⁻² by changing the growth regimes. Third, annealing at $T=480-625$ °C was employed to modify the size and composition of the Ge islands, which was expected to enhance the overlap of carrier wave functions without seriously affecting the e-e interaction in the system. Variation in QD structural parameters was applied to QD arrays with different doping levels. To reveal the influence which the e-e interaction has on the transport behavior of the QD systems under study, we used samples in which the long-range Coulomb potential was screened with a metal plane located close to the QD layer.

The mechanism of charge transport in examined systems was analyzed considering the whole data set taken from samples grown, doped, and annealed under different conditions. As a rule, the transport behavior of 2D systems can be adequately understood within the framework of the theory of quantum corrections¹⁷ (in the range $G > e^2/h$) or within the theory of hopping conduction¹⁸ (in the range $G < 10^{-4}e^2/h$). However, the wide intermediate range of G still remains a matter of heated debates.

For instance, G. M. Minkov *et al.*,¹⁹ who examined the field dependencies of conductance tensor components in low and high magnetic fields, have arrived at a conclusion that all transport phenomena in the systems of interest could be adequately described within the framework of the quantum correction theory even at conductance values much smaller than e^2/h . When analyzing the nonohmic conductance,²⁰ they came to a conclusion that the conductance in 2D systems

behaves such as a diffusion one down to $G \approx 10^{-2}e^2/h$. However, Gershenson *et al.*²¹ showed that in hopping systems with a large radius ξ the behavior of conductance nonlinearity and magnetoresistance is similar to that in WL systems. In such systems, electron motion is still diffusive within the localization domain, with the same electron mean-free-path l as in WL regime.

To discriminate between the hopping and diffusion regimes in our samples, in the present work we thoroughly examined the conductance versus temperature within the strong and weak localization approaches, and also analyzed the conductance nonlinearity, using the method proposed in Ref. 20. As a result, we identified a transition from hopping to diffusion transport, and the range of intermediate conductance values was found to be much narrower ($10^{-2}e^2/h \leq G \leq 0.4e^2/h$) than that known from previously reported experimental data.

When checking the scaling hypothesis for our samples, we found that both the interaction and the disorder determine the transport mode of the system and the transition from strong to weak localization. With the interaction force changing insignificantly, data taken from samples with different QD array densities and from samples annealed at different conditions can be described with one-parameter scaling practically for all used filling factors. The only sample in which the interaction reaches a maximum value ($\nu=2$) exhibited an upward shift of the Gell-Mann-Low function² from the common curve for all other samples, suggesting that the interaction is the second parameter determining the system state. The role of the long-range Coulomb interaction is definitely confirmed by the observation of downward shift of the universal scaling curve in the case when the interaction is screened by the metal plane located nearby of the QDs plane.

The paper is organized as follows. The samples and the experimental conditions are described in Sec. II. The analysis of the conductance versus temperature is given in Sec. III. The nonlinearity study for the conductance is reported in Sec. IV. Finally, the scaling behavior of examined QD arrays is discussed in Sec. V.

II. SAMPLES AND EXPERIMENT

The samples were grown on a (001) *p*-Si substrate with a resistivity of 20 $\Omega \cdot \text{cm}$ by molecular-beam epitaxy of Ge in the Stranskii-Krastanov growth mode. There were two regimes of growth allowing to obtain the QDs array with different density. In the first case, the growth temperature for 10 monolayers (ML) Ge layer was 300 °C and the growth rate was 0.2 ML/s. As a result, the areal density of the dots was shown to be $\sim 4 \times 10^{11}$ cm⁻². This type of samples we named as single density (SD) samples. In the second case, decrease in the Ge growth temperature down to 275 °C with simultaneous increase in the growth rate allows to reach the twice higher QDs areal density ($\sim 8 \times 10^{11}$ cm⁻²). These samples we refer to as double density (DD) samples. To supply holes to the dots, a boron δ -doped Si layer was inserted 5 nm below the Ge QDs layer. Because the ionization energy of boron impurities in Si is 45 meV and the energies of the first ten hole levels in Ge QDs of this size are 200–400

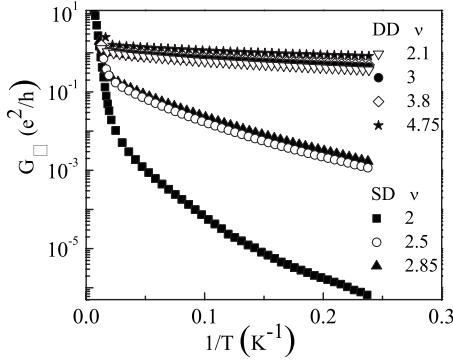


FIG. 1. Temperature dependence of conductance for the samples with different areal density and filling factor ν .

meV,²² at low temperatures holes leave impurities and fill levels in QDs. To get significant changes of the localization radius ξ , the number of holes per dot was chosen to be 2, 2.5, and 2.85 for the SD samples and 2.1, 3, 3.8, and 4.75 for the DD samples. The SD samples were exposed to additional annealing in Ar atmosphere during 30 min at 550, 575, 600, and 625 °C. The silicon cap layer has a thickness of 40 nm. Al metal source and drain electrodes were deposited on the top of structure and heated at 480 °C to form reproducible Ohmic contacts. The resistance along the QDs layer was measured by the two-terminal method with a Keithley 6514 electrometer. The temperature stability was controlled using Ge thermometer. The conductance measurements were carried out using transport dewar at temperatures from 300 to 4.2 K and in voltage range of 0.1 to 10 V.

III. TEMPERATURE DEPENDENCE OF CONDUCTIVITY

Typical temperature dependencies of conductance $G_{\square}(T)$ in e^2/h units are shown in Fig. 1 as Arrhenius plots for nonannealed SD and DD samples with different dot filling factor.

One can see that the conductance of SD sample is much less than that for DD sample and changes with the filling factor ν . The G values of DD samples lie in the range typical for the diffusive regime.²³ Dependence of $G(\nu)$ for the sample with QDs double density is very weak and monotonous. Annealing of all SD samples at 550–625 °C leads to an increase in the conductance with annealing temperature. Typical curves after this treatment are shown in Fig. 2 for the SD sample with $\nu=2.5$. The conductance of this sample reaches $G \sim e^2/h$ after treatment at 600–625 °C; for the sample with $\nu=2.85$ conductance tends to $G \sim e^2/h$ after 625 °C annealing, whereas the G of the sample with $\nu=2$ always remains much less than e^2/h .

A. Analysis in the framework of hopping transport

In general, the temperature dependence of conductance for variable-range hopping (VRH) is given by

$$G(T) = \gamma T^m \exp[-(T_0/T)^x], \tag{1}$$

where γ and m are the constants, T_0 is the material-dependent constant, $x=1/3$ (Mott law) and $x=1/2$ [Efros-

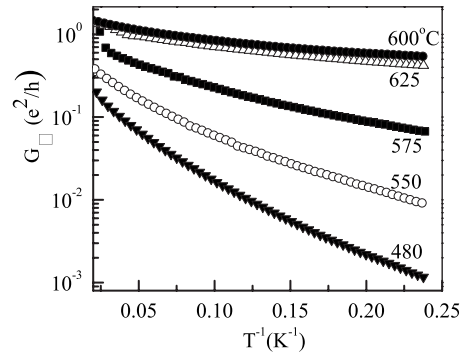


FIG. 2. Temperature dependence of conductance for the SD samples with $\nu=2.5$ annealing at 480–625 °C.

Shklovskii (ES) law] for the 2D VRH without and with electron-electron interaction, correspondingly. When $m \sim 0$, the prefactor becomes temperature independent and phononless hopping with universal conductivity prefactor $G_0 \sim e^2/h$ is observed. Phononless mechanism of hopping conduction was proposed in ref.^{24,25} and involves the stimulation of the electron transition between localized states by a charge fluctuation in close located pairs—fluctuators.

Localization length ξ can be determined for interacting samples from the T_0 value as $\xi = Ce^2/\epsilon k_B T_0$, where theoretical value of constant C for single-electron hopping²⁶ in 2D is $C=6.2$, and ϵ is the static dielectric response, k_B is the Boltzmann’s constant. To determine the behavior of $G(T)$, we analyze the temperature dependence of the reduced activation energy $w(T) = \partial \ln G(T) / \partial \ln T = m + x(T_0/T)^x$ using the method proposed in Ref. 27. In this approach, if $m \ll x(T_0/T)^x$, then $\ln w(T) = A - x \ln T$ and $A = x \ln T_0 + \ln x$. Plotting $\ln w$ as a function of $\ln T$, one can find the hopping exponent x from the slope of the straight line. The parameter A can be found by the intersection point of the straight line with the ordinate axis, which gives the characteristic temperature $T_0 = (10^{A/x})^{1/x}$. Typical plot of $\ln w$ versus $\ln T$ for the SD sample with $\nu=2.5$ annealed at different temperatures are given in Fig. 3. When linear relationship is observed between $\ln w(T)$ and $\ln(T)$, it means that $m \ll x(T_0/T)^x$ and

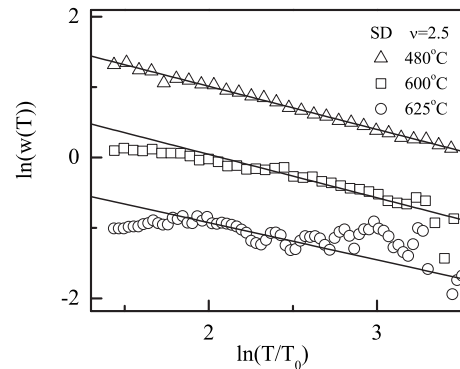


FIG. 3. Analysis of the reduced activation energy for SD sample with $\nu=2.5$ annealed at 480–625 °C. The solid lines are least-squares fits to the linear dependence. Data oscillations for the sample annealed at 625 °C are an artifact that can be defined by temperature or conductance fluctuation during the measurements.

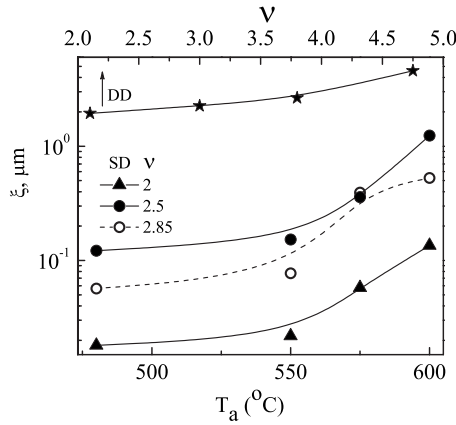


FIG. 4. Localization length ξ for SD samples with different ν annealed at 480–600 °C (bottom curves) and for DD samples in dependent on ν (top curve) without additional annealing. The lines are provided as a guide to the eye.

parameter x can be determined. Analysis of all used samples shows that the SD samples annealed at the temperature up to 575 °C are well described by the Eq. (1) with $x \approx 0.5 \pm 0.05$, typical for the ES law. The exponent m was extracted from the fitting of the experimental dependencies of $G(T)$ with Eq. (1). We have obtained $m \sim 0.1$ for these samples, which indicate that in the samples with the Coulomb gap the pre-exponential factor is virtually temperature-independent and conductance is determined by the phononless hole hopping. The $G(T)$ for the DD samples and for SD samples with $\nu=2.5$ and 2.85 annealed at 600–625 °C is possible to describe by the same equation but with poor accuracy. Nevertheless, the same procedure was carried out for all samples and both T_0 and localization length ξ were determined.

The ξ values for all SD samples annealed at 480–600 °C are shown in a Fig. 4.

After 480 °C treatment the magnitude of ξ is about of 18 and 120 nm for the sample with $\nu=2$ and 2.5, correspondingly. The consequent heating leads to the increase in ξ for all SD samples, but the rate of this increase is much larger for the sample with $\nu=2.5$. After 625 °C annealing of SD samples, as well as for all DD samples (Fig. 4, top curve) the formally determined values of ξ are about some micrometers.

In the samples with large ξ the criterion $r_h \gg \xi$ (here $r_h = \xi(T_0/T)^x$ —the hopping length) for the hopping transport is violated because of the $T_0 (\sim 4-12 \text{ K}) \sim T$. The large ξ magnitude, poor accuracy in the evaluation of $G(T)$ by the VRH, high value of conductance ($\sim e^2/h$), and weak temperature dependence of conductance suggest that the theory of quantum correction can be applied for describing the transport behavior in this kind of samples.

B. Weak localization approach

In the classical case, the conductance in diffusive regime is described by Drude formula and does not depend on the temperature. The quantum corrections to the conductance due to the interference of elastically scattered electrons lead to the logarithmic decrease in the conductance with decrease

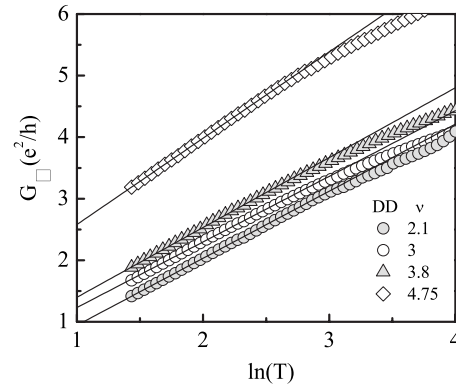


FIG. 5. Conductance of DD samples in dependent on $\ln T$. Lines are the logarithmic approximations of the experimental data.

ing temperature. For the 2D case this correction gives the additional negative contribution $\Delta G \approx -2(e^2/h)\ln(L_\phi/l)$,¹⁶ where l is the electron mean-free path and L_ϕ is the phase break length, $L_\phi \sim T^\alpha$, $\alpha < 0$. As the result, $\Delta G \propto \ln T$. It was shown^{17,28} that the same dependence of $\Delta G(T)$ appears due to the influence of the interaction.

The temperature dependencies of all investigated samples were analyzed in the frame of the theory of quantum corrections. Figure 5 shows the conductance versus $\ln T$ for the DD samples. One can see that the conductance is well described by the logarithmic law up to 20K and $\Delta G \sim 1 \div 4 \times 10^{-5} \text{ } \Omega^{-1}$ that is a typical value for the quantum corrections.²⁹ As for SD samples, the $G(T)$ dependencies fall into the logarithmic law for the sample with $\nu=2.5$ only after annealing at $T \geq 600$ °C and for the sample with $\nu=2.85$ after annealing at 625 °C. Logarithmic temperature dependence of conductance testifies to the transition to the weak localization behavior after the annealing of the samples with such nonwhole filling factors. The SD sample with $\nu=2$ never shows the $\Delta G \propto \ln T$ dependence and the conductance of this sample is changed in some orders with temperature (Fig. 6). Such a behavior is not a typical for the weak localization regime, in which ΔG should be of the same order as the conductance itself.²⁹

Thus, the hopping transport and quantum correction approaches give noncontradictory description of conductance

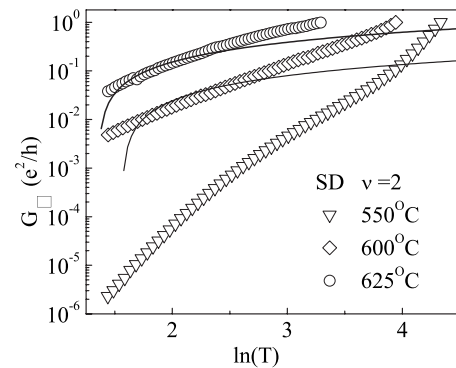


FIG. 6. Conductance of SD samples with $\nu=2$ annealed at different temperatures as a function of $\ln T$. Lines are the logarithmic approximations of the experimental data.

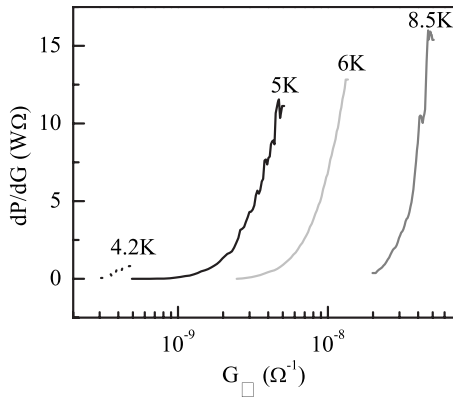


FIG. 7. The relative nonlinearity as a function of conductance measured at different lattice temperature for the SD samples with $\nu=2$ after annealing at 550 °C.

regimes and allow to distinguish samples with strong and weak localization behavior.

IV. NONLINEARITY OF CONDUCTIVITY

In the conventional hopping regime, the nonlinear effects are usually associated with “tilting” of electron hops³⁰ in an electric field $E > k_B T / e r_h$. The nonlinear effects in diffusive transport are caused by electron heating³¹ and determined by the electron temperature T_e only. Starting from these differences, authors²⁰ proposed the method allowing to divide the hopping and diffusive transport regimes. This method is based on the analysis of power density Q injected to the sample. It was shown that the function of relative nonlinearity introduced as $\eta = \frac{\partial G(Q)/\partial Q}{\partial G(T)/\partial T} \Big|_{G(Q)=G(T)} = \frac{(\partial G(T)/\partial T_e)(\partial T_e/\partial Q)}{\partial G(T)/\partial T}$ and measured at different temperatures can determine the transport behavior. As long as the conductance remains diffusive, the T_e —dependencies of η measured at different lattice temperatures T_l have to fall on common curve and this property has to disappear when the conductance becomes hopping. Since $\partial G/\partial T$ for the diffusive case equal to $\partial G/\partial T_e$, the same results should be valid for the analysis of dQ/dT instead of $\eta(T)$ and correspondingly, for the analysis of the derivative dP/dT of full power P injected to the sample. To write $dP/dT = (\partial P/\partial G)(\partial G/\partial T)$ and to take into account that $\partial G/\partial T$ depends only on temperature, experimentally we studied the dP/dG versus G . Such dependences was examined for two SD samples with $\nu=2$ annealed at 550 °C and with $\nu=2.5$ annealed at 625 °C. As noted before, the temperature dependence of conductance for the first sample corresponds to the hopping regime, for the second one is well described by the quantum corrections to the conductance.

To obtain the dP/dG , we measured IV characteristics in nonohmic regime, determined $P=IV$ and $G=I/V$ and than numerically differentiated the $P(G)$ dependence. The results of such a procedure are shown in the Figs. 7 and 8 for the first and second samples, correspondingly. Inset to Fig. 8 shows the IV characteristics of the sample measured at different temperatures. One can see that the dP/dG versus G data obtained for different lattice temperatures fall on a common curve for the high-conductance sample with logarithmic

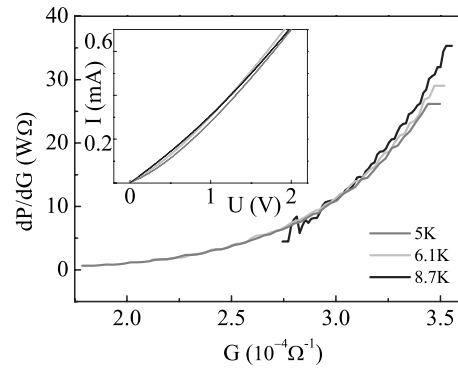


FIG. 8. The relative nonlinearity as a function of conductance measured at different lattice temperatures for the SD sample with $\nu=2.5$ after annealing at 625 °C. Inset demonstrates initial IV characteristics measured at different temperatures.

temperature dependence of G (Fig. 8). On a contrary, for the sample in which the temperature dependence of G described by VRH, the approximation of the electron temperature fails (Fig. 7). It means that the conductance is defined by both electron and lattice temperature due to the increase in the hopping probability and impact ionization that is the characteristic feature of hopping behavior. In the case of the phononless transport the lattice temperature determines the hopping probability in close located pairs fluctuators. The result of the nonlinear conductance analysis confirms the transport behavior of the system determined from the measurements of the $G(T)$ dependencies and testifies to the crossover from hopping to diffusive transport in quantum dots array annealed at high temperature.

V. SCALING HYPOTHESIS

To check whether one- or two-parameter scaling correctly describes our system, we analyzed the $G(T)$ dependencies of all used samples in the frame of classical scaling theory. The idea of scaling hypothesis was proposed in Ref. 2 for the description of the metal-insulator transition. Following this approach, the single scaling parameter—conductance, can be used to describe the system state. They choose the Gell-Mann-Low function $\beta(G) = d \ln(G) / d \ln(L)$ (L is the sample size), which is the universal one for every dimension and depends only on the conductance itself. On a metallic side of transition $\beta = d - 2$ (d is the system dimension), and $\beta \propto \ln(G)$ on the insulator side.

It can be shown (see Appendix) that in the case of the universal $\beta(\ln G)$ dependence, the universality should remain also for $\ln G$ versus $\ln T$ one after rescaling the temperature axis. Moreover, when the conductance range for set of samples is not too large, to use the scaling for $\ln G$ is more suitable than that for derivative.

The $\ln(G/G_0)$ versus $\ln(T/T_s)$ is plotted in a Fig. 9 for all SD and DD samples under study. T_s is the arbitrary value, chosen in our case as 1 K. We find that by rescaling the temperature axis for each sample all of the data can be made to overlap on a single smooth trajectory shown as a black line. It is remarkable that a single scaling trajectory works

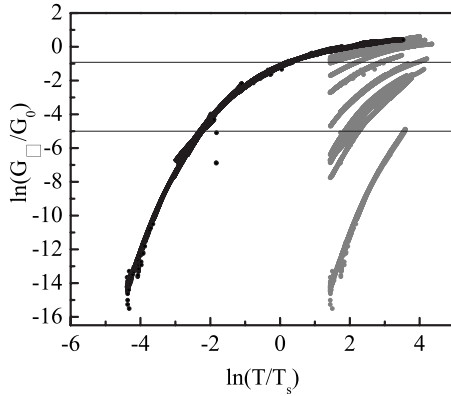


FIG. 9. Temperature dependencies of conductivity for all used SD and DD samples (gray curves). Black universal curve obtained by rescaling of the T axis. Lines divide the diffusion and hopping behavior.

for the samples with different structural parameters, different QDs density, treated in different regimes, with and without additional annealing. The conductance as a function of temperatures at the extremes should correspond to weak localization behavior for the high-conductance regime and to the hopping transport for low-conductance one. To check that and find the bounds that separate two regimes, we approximated the universal dependence by both $G \sim \ln(T)$ and $G \sim \exp(T_0/T)^{0.5}$. The results of such an approximation are shown in the Figs. 10 and 11, correspondingly. One can see that at $G \leq 10^{-2}e^2/h$ the conductance in the system is well described by the hopping transport, whereas at $G \geq 0.4e^2/h$ the conductance is due to the diffusive one. At that hopping regime defines the behavior of SD samples annealed at 480 °C with different filling factor, while conductance of DD samples and SD samples annealed at 600–625 °C falls into diffusive regime. The observed range for intermediate conductance is significantly narrower as compared with previous experimental data.

To find the inferred deviation from the universal curve due to interaction, we carried out the analysis of $\ln G$ derivative (β function). As it was shown in Appendix, for the hopping case β function can be represented as

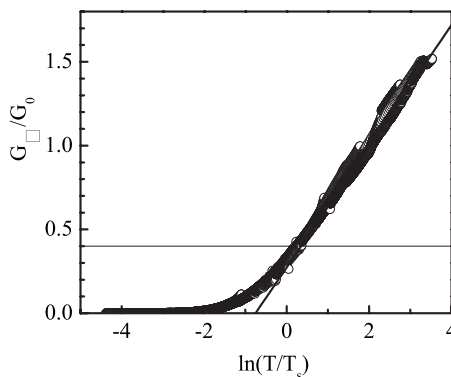


FIG. 10. The logarithmic approximation of the universal curve for high-conductance samples from Fig. 9. Line separates the weak localization regime.

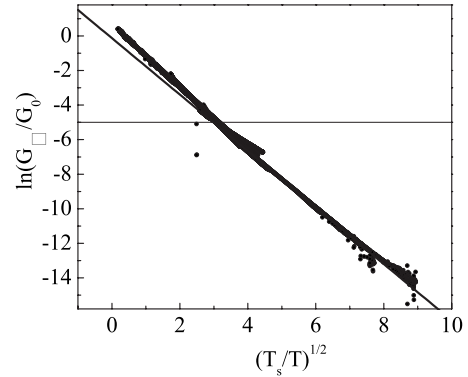


FIG. 11. The ES-law approximation of the universal curve for low-conductance samples from Fig. 9. Line separates the hopping regime.

$$\beta = \frac{1}{2.3x} \left(- \frac{d \ln G}{d \ln T} \right). \quad (2)$$

The β versus $\ln G$ dependencies are analyzed for the samples with hopping transport behavior and the results are shown in Fig. 12. The middle curve demonstrates the results of β calculations for the samples with different filling factor of dots with holes, different structural parameters of dots, and after different annealing of samples. The only sample with $\nu=2$ has an upward deviation from this universal curve. The value of this shift can be characterized by the change in conductance value at the same magnitude of β function. For the sample with $\nu=2$ conductance decreases by a factor of ten as compared to the samples with all other doping levels. We suggest that namely Coulomb interaction that reaches the maximum value at full filling of QDs ground state ($\nu=2$) can be a second parameter besides the conductance that determined the system behavior. To rewrite the expression (2) using the temperature dependence $G(T) = G_1 \exp[-(T_0/T)^{0.5}]$

$$\beta = \frac{1}{2.3} \ln(G_0/G_1) + \frac{1}{2.3} \ln(G/G_0), \quad (3)$$

we can see that the pre-exponent term G_1 is the factor responsible for the shift of the universal curve. The nonmonotonic change in G_1 versus filling factor of holes in QDs in the wide range of ν variation (0.5–6 holes per dot) was demon-

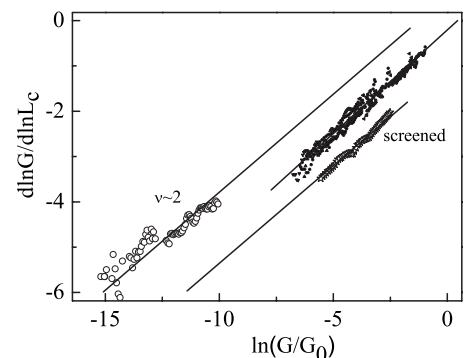


FIG. 12. β function for the samples under study.

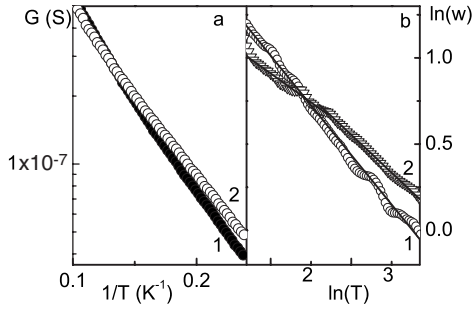


FIG. 13. Temperature dependence of conductance (a) and the logarithmic derivative $\ln(w)$ (b) for unscreened (1) and screened (2) samples.

strated by Yakimov¹⁴ for the samples exhibiting phononless hopping transport.

To obviously check the influence of long-range interaction to the system behavior, we use the screening of the interaction putting a metal plate on the vicinity of QDs parallel to the dot layer. The details of this procedure are described in Ref. 32. The temperature dependencies of the conductance for the samples with and without screening is shown in the Fig. 13(a).

The analysis of the reduced activation energy for two samples [Fig. 13(b)] testifies to the crossover from the interaction driven hopping (ES law) to the Mott one at temperatures smaller than 9K. It means that the metal plane effectively screens the long-range Coulomb interaction in this system. Moreover, we already shown³² that transition from ES to Mott VRH is accompanied by the simultaneous transfer from electron to phonon-assisted hopping.

The β function for both unscreened (inside the middle curve) and screened samples (bottom curve) is added to Fig. 12. One can see that the β of sample with screening Coulomb interaction downwards from the middle curve. This shift corresponds to the conductance value five times more than that for unscreened samples at the same magnitude of the β function. This result is a direct indication that not only disorder but also interaction determines the system behavior and confirms two-parametric scaling in interacting 2D systems. Independent contribution of these parameters into scaling has never been observed experimentally before.

VI. CONCLUSIONS

Using different methods for the variation in the disorder and interaction, the effect of the long-range interaction on the transport in two-dimensional QD structures was revealed experimentally. It was shown that in the case of negligible changes of the interaction force the transport properties of samples with different QD array densities and samples annealed at different conditions could be adequately described with the Gell-Mann-Low one-parameter scaling function. Upward deviation of the universal curve is observed in the

QD structures with filling factor $\nu=2$, for which the interaction reaches a maximum value, whereas the screening of the Coulomb interaction leads to the downward shift of this curve. Five times more change in conductance is observed for the screened sample as compared with the unscreened one at the same value of β function. It was found that at $G \leq 10^{-2} e^2/h$ the conductance in the system is well described by the hopping transport, the diffusive regime is observed at $G \geq 0.4 e^2/h$. The crossover from strong to weak localization behavior takes place at the increase in QDs density and annealing of samples with nonwhole filling factor at 600–625 °C.

ACKNOWLEDGMENTS

We give thanks to A.G. Pogosov, A.L. Burin, A. V. Nenashev, and A.I. Yakimov for useful discussions. This work was supported by RFBR (Grant No. 08-02-12095).

APPENDIX

The function β in classical scaling theory is determined at $T=0$. When the correlation length L_c determining the conductance both in insulator and metallic phase becomes finite ($T \neq 0$) and $L > L_c$, it is correct to use L_c derivative instead of L one. In this case the conductance of L —size sample can be represented as a sum of the series and parallel resistances with the L_c —size. It is obvious that $G(L)=G(L_c)$ and $\beta = d \ln(G)/d \ln(L) = d \ln(G)/d \ln(L_c)$. Thus, instead of the sample size variation we can turn into the variation in the L_c . The simplest way to change the L_c is the changing of the temperature. For the hopping case, the L_c is the correlation radius of the percolation network $L_c \sim \xi(T_0/T)^{x(1+\alpha)}$, where α ($=1.3$ for 2D) is the corresponding critical index and $x=1/3$ (Mott law) and $x=1/2$ (ES law) (see above Eq. (1)). For the diffusion regime, $L_\varphi \sim 1/T^{0.5}$. Suggesting $L_{c,\varphi}(T)$ dependence, the β can be written down as

$$\beta = \frac{d \ln G}{d \ln L_{c,\varphi}} = \frac{d \ln G}{d \ln T} \frac{d \ln T}{d \ln L_{c,\varphi}}.$$

Hence,

$$\beta(G) = \frac{d \ln G}{d \ln L_{c,\varphi}} = \gamma_{1,2} \frac{d \ln G}{d \ln T},$$

where $\gamma_{1,2}$ are proportional to the corresponding exponents in $L_{c,\varphi}(T)$ dependencies. Represent this expression as:

$$\frac{d \ln G}{\gamma_{1,2} \beta(G)} = d \ln T,$$

after its integration one can obtain that $f(\ln G) = \ln T + C$, here C is a constant. Hence, we have shown that $\ln G(\ln T)$ curves should be universal after rescaling the temperature axis.

*stepina@isp.nsc.ru

- ¹P. W. Anderson, Phys. Rev. **109**, 1492 (1958).
- ²E. Abrahams, P. W. Anderson, D. C. Licciardello, and T. V. Ramakrishnan, Phys. Rev. Lett. **42**, 673 (1979).
- ³S. V. Kravchenko, Whitney E. Mason, G. E. Bowker, J. E. Furneaux, V. M. Pudalov, and M. D'Iorio, Phys. Rev. B **51**, 7038 (1995).
- ⁴M. Y. Simmons, A. R. Hamilton, M. Pepper, E. H. Linfield, P. D. Rose, D. A. Ritchie, A. K. Savchenko, and T. G. Griffiths, Phys. Rev. Lett. **80**, 1292 (1998).
- ⁵D. Simonian, S. V. Kravchenko, M. P. Sarachik, and V. M. Pudalov, Phys. Rev. Lett. **79**, 2304 (1997).
- ⁶A. M. Finkel'shtein, JETP Lett. **37**, 517 (1983); Sov. Phys. JETP **57**, 97 (1983); **59**, 212 (1984); A. M. Finkel'stein, Z. Phys. B: Condens. Matter **56**, 189 (1984).
- ⁷A. Punnoose and A. M. Finkel'stein, Science **310**, 289 (2005).
- ⁸E. Abrahams, S. V. Kravchenko, and M. P. Sarachik, Rev. Mod. Phys. **73**, 251 (2001).
- ⁹G. Benenti, X. Waintal, and J.-L. Pichard, Phys. Rev. Lett. **83**, 1826 (1999).
- ¹⁰G. Katomeris, F. Selva, and J.-L. Pichard, Eur. Phys. J. B **31**, 401 (2003).
- ¹¹D. A. Knyazev, O. E. Omel'yanovskii, V. M. Pudalov, and I. S. Burmistrov, Phys. Rev. Lett. **100**, 046405 (2008).
- ¹²S. Anissimova, S. V. Kravchenko, A. Punnoose, A. M. Finkel'stein, and T. M. Klapwijk, Nat. Phys. **3**, 707 (2007).
- ¹³A. I. Yakimov, A. V. Dvurechenskii, V. V. Kirienko, Yu. I. Yakovlev, A. I. Nikiforov, and C. J. Adkins, Phys. Rev. B **61**, 10868 (2000).
- ¹⁴A. I. Yakimov, A. V. Dvurechenskii, A. V. Nenashev, and A. I. Nikiforov, Phys. Rev. B **68**, 205310 (2003).
- ¹⁵A. I. Yakimov, A. V. Dvurechenskii, A. I. Nikiforov, and A. A. Bloshkin, JETP Lett. **77**, 376 (2003).
- ¹⁶L. P. Gor'kov, A. L. Larkin, and D. E. Khmel'nitskii, Pis'ma Zh. Eksp. Teor. Fiz. **30**, 248 (1979) [JETP Lett. **30**, 228 (1979)].
- ¹⁷B. L. Altshuler and A. G. Aronov, in *Electron-Electron Interaction in Disordered Solids*, edited by A. L. Efros and M. Pollak (North-Holland, Amsterdam, 1985).
- ¹⁸B. I. Shklovskii and A. L. Efros, *Electronic Properties of Doped Semiconductors*, Springer Series in Solid-State Sciences (Springer-Verlag, New York, 1984).
- ¹⁹G. M. Minkov, O. E. Rut, A. V. Germanenko, A. A. Sherstobitov, B. N. Zvonkov, E. A. Uskova, and A. A. Birukov, Phys. Rev. B **65**, 235322 (2002).
- ²⁰G. M. Minkov, A. A. Sherstobitov, O. E. Rut, and A. V. Germanenko, Physica E **25**, 42 (2004).
- ²¹M. E. Gershenson, Yu. B. Khavin, D. Reuter, P. Schafmeister, and A. D. Wieck, Phys. Rev. Lett. **85**, 1718 (2000).
- ²²A. V. Dvurechenskii, A. V. Nenashev, and A. I. Yakimov, Nanotechnology **13**, 75 (2002).
- ²³Z. Ovadyahu and Y. Imry, Phys. Rev. B **24**, 7439 (1981).
- ²⁴V. I. Kozub, S. D. Baranovskii, and I. Shlimak, Solid State Commun. **113**, 587 (2000).
- ²⁵A. L. Burin and L. A. Maksimov, Sov. Phys. JETP **95**, 1345 (1989).
- ²⁶D. N. Tsigankov and A. L. Efros, Phys. Rev. Lett. **88**, 176602 (2002).
- ²⁷A. G. Zabrodskii and K. N. Zinoveva, Zh. Eksp. Teor. Fiz. **86**, 727 (1984) [Sov. Phys. JETP **59**, 425 (1984)].
- ²⁸P. A. Lee and T. V. Ramakrishnan, Rev. Mod. Phys. **57**, 287 (1985).
- ²⁹V. F. Gantmakher, *Electrons in Non-Ordered Medium* (Fizmatlit, Moscow, 2003).
- ³⁰B. I. Shklovskii *et al.*, in *Transport, Correlations and Structural Defects*, edited by H. Fritzsche (World Scientific, Singapore, 1990), p. 161.
- ³¹M. Henny *et al.*, Appl. Phys. Lett. **71**, 773 (1997).
- ³²N. P. Stepina, E. C. Koptev, A. V. Nenashev, A. V. Dvurechenskii, and A. I. Nikiforov, Phys. Status Solidi C **5**, 689 (2008).